

## Nature of the Band Gap of $\text{In}_2\text{O}_3$ Revealed by First-Principles Calculations and X-Ray Spectroscopy

Aron Walsh,<sup>1,\*</sup> Juarez L. F. Da Silva,<sup>1</sup> Su-Huai Wei,<sup>1</sup> C. Körber,<sup>2</sup> A. Klein,<sup>2</sup> L. F. J. Piper,<sup>3</sup> Alex DeMasi,<sup>3</sup> Kevin E. Smith,<sup>3</sup> G. Panaccione,<sup>4</sup> P. Torelli,<sup>5</sup> D. J. Payne,<sup>6</sup> A. Bourlange,<sup>6</sup> and R. G. Egdell<sup>6</sup>

<sup>1</sup>National Renewable Energy Laboratory, Golden, Colorado 80401, USA

<sup>2</sup>Darmstadt University of Technology, 64287 Darmstadt, Germany

<sup>3</sup>Department of Physics, Boston University, 590 Commonwealth Avenue, Boston, Massachusetts 02215, USA

<sup>4</sup>Laboratorio TASC, INFN-CNR, Area Science Park, S.S. 14, Km 163.5, 34012 Trieste, Italy

<sup>5</sup>CNR-INFN-S3, Via Campi 213/A, I-41100 Modena, Italy

<sup>6</sup>Chemistry Research Laboratory, Mansfield Road, Oxford OX1 3TA, United Kingdom

(Received 5 November 2007; published 25 April 2008)

Bulk and surface sensitive x-ray spectroscopic techniques are applied in tandem to show that the valence band edge for  $\text{In}_2\text{O}_3$  is found significantly closer to the bottom of the conduction band than expected on the basis of the widely quoted bulk band gap of 3.75 eV. First-principles theory shows that the upper valence bands of  $\text{In}_2\text{O}_3$  exhibit a small dispersion and the conduction band minimum is positioned at  $\Gamma$ . However, direct optical transitions give a minimal dipole intensity until 0.8 eV below the valence band maximum. The results set an upper limit on the fundamental band gap of 2.9 eV.

DOI: 10.1103/PhysRevLett.100.167402

PACS numbers: 78.70.En, 73.20.At, 78.20.Bh

Despite the widespread use of  $\text{In}_2\text{O}_3$  as a transparent contact in photovoltaic devices, liquid crystal displays, and light emitting diodes [1,2], the nature of the band gap in this material remains contentious [3–6]. Early measurements on  $\text{In}_2\text{O}_3$  single crystals showed that the onset of strong optical absorption is found to be 3.75 eV, but with indications of a much weaker absorption onset at 2.62 eV attributed to indirect electronic transitions [7]. Nonetheless the “band gap” of  $\text{In}_2\text{O}_3$  is widely quoted as 3.75 eV [8] or thereabouts [9]. However, the top of the valence band in x-ray photoemission spectra of lightly doped *n*-type  $\text{In}_2\text{O}_3$  is found to be *less* than 3 eV below the Fermi level (which is situated just above the bottom of the conduction band), adding further weight to the hypothesis that  $\text{In}_2\text{O}_3$  may have an indirect band gap [10]. It has been argued [5] that an indirect gap could arise from mixing of shallow core In *4d* states with O *2p* states away from the  $\Gamma$  point within the centrosymmetric crystal structure of  $\text{In}_2\text{O}_3$ : a similar situation pertains in rocksalt CdO where the lowest energy gap is undoubtedly indirect [5,11]. However, band structure calculations [3] on  $\text{In}_2\text{O}_3$  have consistently failed to find upward dispersion of the topmost valence band by the 1 eV required by the indirect gap hypothesis. It has therefore been argued that the onset of valence band photoemission intensity is reduced from the value expected on the basis of the bulk band gap by upward band bending at the surface and that the weak optical absorption around 2.6 eV is associated with defects [4,6].

In this Letter we compare the positions of valence band edges in conventional x-ray photoemission spectra with those measured with the very much less surface sensitive techniques of hard x-ray photoemission and x-ray emission spectroscopies (XPS and XES): while the valence electron inelastic mean free path length in Al *K $\alpha$*  XPS is probably of the order of 25 Å, under 6000 eV excitation the path

length increases to values around 60 Å [12]. XES is a photon-in photon-out technique with an effective sampling depth of order 1000 Å. We find that there is no significant shift in spectral features between the different experimental techniques, which argues strongly against the band bending model. Moreover we further demonstrate, through symmetry analysis of the band structure, that direct optical transitions at  $\Gamma$  from the valence band maximum (VBM) to the conduction band minimum (CBM) are parity forbidden and that the first strong transitions occur from valence bands 0.81 eV *below* the VBM. This new insight solves the long-standing “band gap discrepancy” and calls for a reinterpretation of all experimental and theoretical studies of  $\text{In}_2\text{O}_3$  that require knowledge of the fundamental gap.

$\text{In}_2\text{O}_3$  and Sn-doped  $\text{In}_2\text{O}_3$  (2% and 10 weight % Sn) were deposited by radio frequency magnetron sputtering onto doped Si substrates to a thickness of 400–500 nm using pure Ar as the sputter gas and a 400 °C substrate temperature. Carrier concentrations were estimated from conductivity values using a mobility of 30 cm<sup>2</sup> V<sup>-1</sup> s<sup>-1</sup> and from measured energies of plasmon satellites on In *3d* core lines [10]. For the most highly doped sample the carrier concentration reaches a value of  $1.2 \times 10^{21}$  cm<sup>-3</sup>. Conventional x-ray photoemission spectra were measured *in situ* in the deposition system with a Physical Electronics Phi 5700 spectrometer and *ex situ* with monochromatic Al *K $\alpha$*  radiation ( $h\nu = 1486.6$  eV) in both a Scienta XPS system (incorporating a rotating anode Al *K $\alpha$*  x-ray source and a 300 mm mean radius electron energy analyzer) with an overall energy resolution of 0.35 eV and a VG ESCALAB 250. Energies were referenced relative to Fermi level onsets of Ag samples used to calibrate the spectrometers. The silver Fermi level was found to coincide with weak but well-defined Fermi edges found for the doped  $\text{In}_2\text{O}_3$  samples. Further Al *K $\alpha$*  measurements were

performed on (001) oriented single crystal thin film samples grown by O-plasma assisted molecular beam epitaxy on Y-doped  $\text{ZrO}_2$  substrates. The positions of the valence band onsets were consistent between all the different data sets. Hard x-ray photoemission spectra (HXPS) at  $h\nu = 6000$  eV were measured on beam line 16 at the ESRF [12] again with an overall energy resolution of 0.35 eV. Here spectra were referenced to the Fermi energies of the Sn-doped samples. Finally x-ray emission spectra at the O  $K$  edge were measured at the soft x-ray undulator beam line X1B at the National Synchrotron Light Source (NSLS), Brookhaven National Laboratory. The emission spectra were obtained using a Nordgren-type grazing incidence spherical grating spectrometer with an energy resolution set to 0.35 eV at the O  $K$  edge [13]. The incident photon energy was set far above the absorption threshold at 567 eV. The emission energy axes were calibrated to the second order  $L$  edge of a zinc metal, for the same settings.

The experimental data are shown in Fig. 1. In both Al  $K\alpha$  XPS and HXPS well-defined structure is found close to the Fermi energy which grows in intensity with increasing doping and extends down to about 1.5 eV binding energy in the most highly doped sample. This is associated with occupied conduction band states. The intensity of the conduction band feature increases dramatically relative to the intensity of the valence band edge in switching from excitation at  $h\nu = 1486.6$  eV to  $h\nu = 6000$  eV due to the pronounced In  $5s$  character of the conduction band states and the increasing value of the cross section for In  $5s$  states relative to that for O  $2p$  states with increasing photon energy [14]. The valence band edge is seen to lie 2.9 eV below the Fermi level in both Al  $K\alpha$  XPS and HXPS for the nominally undoped sample and moves to higher binding energies of 3.2 and 3.5 eV, respectively, for 2% and 10% doped samples. All binding energies are referenced to the Fermi level and the shift arises from the upward movement of the Fermi level within the conduction band with increasing doping partially offset by band gap shrinkage with doping. Conduction band occupancy produces the well known Burstein-Moss shift in optical absorption [8]. The magnitudes of the observed band edge shifts are consistent with the known free carrier concentrations [8]. The valence band onset energy of 2.9 eV for the nominally undoped sample sets an upper limit for the fundamental band gap of  $\text{In}_2\text{O}_3$  assuming little or no surface band bending: this value is further reduced by the occupation of conduction band states arising from adventitious donor defects.

A distinct Fermi edge onset was also observed in the x-ray emission spectrum (which is determined by the bulk occupied O  $2p$  like *partial* density of states) of the 10% Sn-doped sample at  $h\nu = 530.06$  eV with a sigmoidal width matching the spectrometer resolution of 0.35 eV. This feature was absent in the spectrum of the nominally undoped sample and allows the x-ray emission data to be transposed onto the same binding energy scale as the

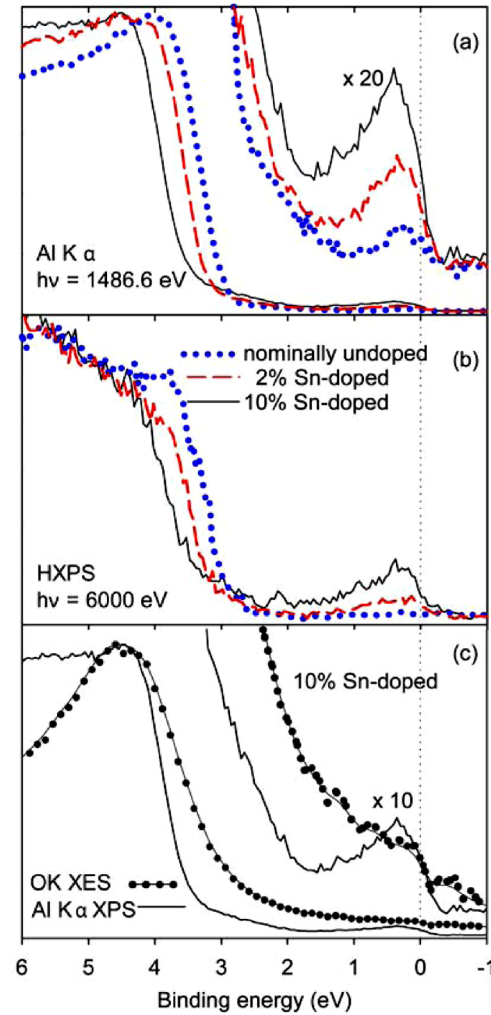


FIG. 1 (color online). (a) Al  $K\alpha$  XPS ( $h\nu = 1486.6$  eV) of nominally undoped and 2% and 10% Sn-doped  $\text{In}_2\text{O}_3$  thin films. (b) HXPS ( $h\nu = 6000$  eV) of the same films. (c) Al  $K\alpha$  XPS and O  $K$  shell XES of 10% Sn-doped  $\text{In}_2\text{O}_3$  aligned using the Fermi edge (0 eV) visible in both spectra.

photoemission data. Although strong band tailing prevents accurate determination of the valence band onset in this spectrum, the valence band peak maximum relative to the Fermi energy is seen to coincide with that in Al  $K\alpha$  XPS. Thus the binding energy scales for all three techniques coincide, a fact which argues strongly against the band bending model.

Similar to  $\text{Ti}_2\text{O}_3$  [15],  $\text{In}_2\text{O}_3$  adopts the body centered cubic bixbyite ( $\text{FeMnO}_3$ ) structure (space group  $Ia\bar{3}$ ,  $T_h^7$  symmetry) with 8 f.u. per primitive cell [16]. Each In atom is coordinated by six oxygen atoms in a distorted octahedron, with In-O interatomic distances ranging from 2.13–2.23 Å and a lattice constant of 10.12 Å [16]. The equilibrium geometric and electronic structure of  $\text{In}_2\text{O}_3$  were calculated using density functional theory [17] within the generalized-gradient approximation [18] (GGA-PBE) and the all electron projector-augmented-wave method [19] as implemented in VASP [20,21]. A plane wave cutoff of

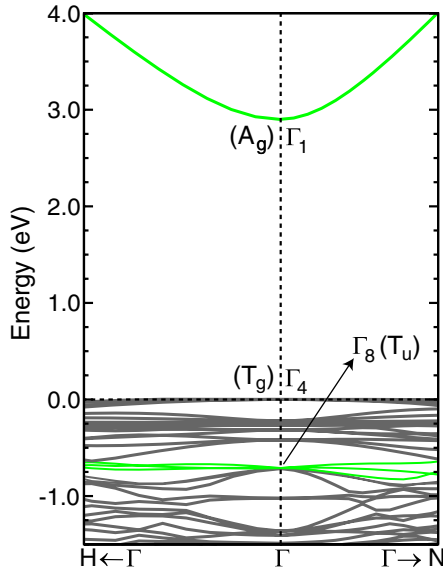


FIG. 2 (color online). Band structure of  $\text{In}_2\text{O}_3$  (along the  $H\text{-}\Gamma\text{-}N$  lines). The highest energy valence bands resulting in strong optical absorption to the conduction band are light gray. A rigid shift of the conduction band is applied to offset the density-functional theory band gap underestimation [22].

400 eV and a  $4 \times 4 \times 4$   $k$ -point mesh were found to give sufficient convergence.

The calculated band structure along two high symmetry lines  $H(1/2, -1/2, 1/2)\text{-}\Gamma(0, 0, 0)\text{-}N(0, 0, 1/2)$  is shown in Fig. 2. The highest occupied band exhibits very little dispersion, e.g., 19 meV along the  $\Gamma\text{-}N$  line. This is clearly inconsistent with the existence of a strongly indirect fundamental gap in the order of 1 eV. The effect of electron correlation on the In  $4d$  states was investigated by using GGA +  $U$  ( $U - J = 5$  eV). The effect is small, resulting in a change of  $\Gamma\text{-}N$  band width of less than 50 meV.

The VBM state at  $\Gamma$  is threefold degenerate and is derived from O  $2p$  and In  $4d$  character ( $\Gamma_4, T_g$  symmetry), while the CBM state is a mixture of In  $5s$  and O  $2s$  orbitals ( $\Gamma_1, A_g$  symmetry). As bixbyite contains an inversion center and the electric-dipole operator is of odd parity, strong optical transitions are only permitted between two states of opposing parity. These symmetry requirements result in a zero optical transition matrix element for direct VBM to CBM absorption at  $\Gamma$ , confirming that this  $\Gamma_4\text{-}\Gamma_1$  transition is formally forbidden and can only make a very weak contribution to photon absorption under the influence of lattice vibrations. It is only from 0.81 eV below the VBM that strong transitions are observed. Here, the wave function character at  $\Gamma$  becomes sufficiently  $p$  like ( $\Gamma_8, T_u$  symmetry) and strong optical transitions can occur, with a transition matrix element of 0.74 a.u. for  $\Gamma_8\text{-}\Gamma_1$  absorption. Five sets of bands lie in the range between 0–0.81 eV, of which three are of even parity, while two are of odd parity; however, while transitions from the odd parity bands at 0.25 and 0.50 eV are nonzero,

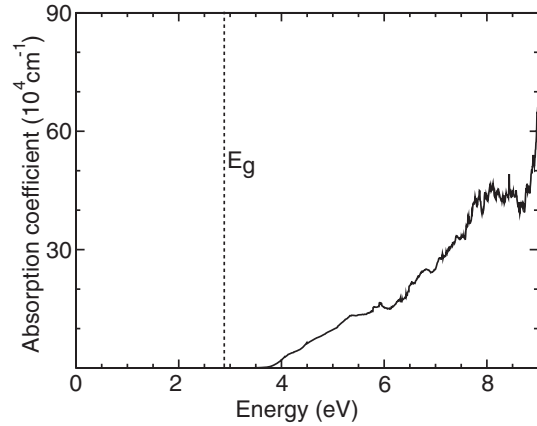


FIG. 3. Calculated absorption spectrum of bulk  $\text{In}_2\text{O}_3$ . Note that the onset of optical absorption is 0.81 eV higher in energy than the fundamental band gap [22].

they result in very small matrix elements on the order of 100 times weaker than the strong  $\Gamma_8\text{-}\Gamma_1$  absorption at 0.81 eV. This is because these states are derived from the “fold-in” bands of the ideal  $\text{In}_2\text{O}_3$  primitive cell, so they are only pseudodirect. Therefore, both the computed optical matrix elements and the resulting absorption coefficient (Fig. 3) are consistent with a fundamental gap 0.81 eV lower in energy than the optical band gap. While the absorption spectrum, summed over all possible direct transitions from a dense sampling of the Brillouin zone, is calculated with a VBM-CBM separation of 2.89 eV [22], the onset of optical absorption is only observed at 3.70 eV, after which the intensity rises with increasing photon energy. This demonstrates that the valence band states within 0.81 eV of the VBM make no significant contribution to low energy photon absorption in the frozen bulk crystal; weak transitions can result experimentally through local symmetry breaking.

$\text{In}_2\text{O}_3$  is the prototypical  $n$ -type transparent conducting oxide [1]. Occupation of the conduction band through  $n$ -type doping, as observed from the increased Fermi energy–VBM separation in the experimental spectra on introduction of Sn (Fig. 1), can induce transitions away from the  $\Gamma$  point due to a Burstein-Moss shift. To take this effect into account theoretically, we have examined the magnitude of the direct optical transitions along the  $H\text{-}\Gamma\text{-}N$  lines. The lowest energy  $\Gamma_4\text{-}\Gamma_1$  transition is parity forbidden, and moving away from the zone center is found to result in no significant increase in the strength of optical transitions. Therefore,  $n$ -type doping will not induce strong absorption below the intrinsic optical gap, which is consistent with the high visible transparency maintained even in heavily doped  $\text{In}_2\text{O}_3$ . As the  $\Gamma_8$  valence band at 0.81 eV below the VBM, which determines the optical gap, exhibits almost no dispersion and the CBM is close to parabolic, there will be a pronounced movement of the absorption onset to higher energies as the conduction band becomes more occupied; this strong shift of the optical gap is well established

experimentally [1,2]. It is also worth noting that in order to preserve simultaneous transparency and conductivity, transitions between the CBM band and other conduction band states near the  $\Gamma$  point must be inhibited. For  $\text{In}_2\text{O}_3$ , this is well obeyed as the CBM + 1 band ( $\Gamma_5$ ) lies 5 eV above the CBM; i.e., the transitions are well outside the visible wavelength range.

We have demonstrated experimentally, using a range of x-ray spectroscopies, that the separation between the VBM and CBM is much less than the previously quoted band gap of 3.75 eV, and is not related to surface band bending; the measurements set an upper limit of 2.9 eV for the fundamental gap. These results are supported by theoretical calculations which conclude that  $\text{In}_2\text{O}_3$  is a “forbidden” gap material with a fundamental band gap 0.81 eV lower in energy than the onset of strong optical absorption. We therefore propose that the weak absorption observed below the optical gap of  $\text{In}_2\text{O}_3$  is a property of the bulk solid, resulting from the formally forbidden transitions at the top of the valence band. Similar symmetry forbidden direct fundamental gaps have been established in other conducting oxide systems including spinel  $\text{SnZn}_2\text{O}_4$ ,  $\text{SnCd}_2\text{O}_4$  and  $\text{CdIn}_2\text{O}_4$  [23],  $\text{CuInO}_2$  [24], cuprite  $\text{Cu}_2\text{O}$  [25], and rutile  $\text{SnO}_2$ ,  $\text{TiO}_2$ , and  $\text{GeO}_2$  [26,27].

These results have wide consequences relating to both the basic understanding of  $\text{In}_2\text{O}_3$  and its applications. For example, the recently observed unusual  $\sim 1.2$  eV redshift in the onset of optical absorption in nitrogen-doped  $\text{In}_2\text{O}_3$  [28] (for the purposes of *p*-type doping) could be explained in terms of the introduction of N  $2p$  levels above the VBM of  $\text{In}_2\text{O}_3$ , breaking the local symmetry and producing a parity allowed transition much higher in energy than the initial optical gap which originates from below the valence band edge. Furthermore, band offsets are generally measured relative to the conduction band or valence band edges, but not both, and thus rely on prior knowledge of the band gap to determine the overall offset. Past estimations of  $\text{In}_2\text{O}_3$  therefore need to be revised; e.g., for  $\text{In}_2\text{O}_3/\text{Si}$  the reported valence band offset of 1.62 eV [29] will be reduced to less than 1 eV.

We are grateful to both G. W. Watson and P. J. Dobson for useful discussions. The work at Golden was supported by the U.S. Department of Energy (DOE) under Contract No. DE-AC36-99GO10337. Work in Darmstadt was supported by DFG Grants No. SFB 595-D3 and No. KL1225/4 and the European Network of Excellence FAME. The Boston University (BU) program was supported in part by DOE under No. DE-FG02-98ER45680 and in part by the donors of the American Chemical Society Petroleum Research Fund. The BU XES/RIXS spectrometer system was funded by the U.S. Army Research Office under No. DAAD19-01-1-0364 and No. DAAH04-95-0014. The NSLS, Brookhaven National Laboratory, is supported by DOE under Contract No. DE-AC02-98CH10886. The Oxford program was supported by EPSRC Grant No. GR/S94148 and the Scienta XPS facility by EPSRC Grant No. EP/E025722/1.

- \*aron\_walsh@nrel.gov
- [1] I. Hamberg and C. G. Granqvist, J. Appl. Phys. **60**, R123 (1986).
  - [2] C. G. Granqvist and A. Hultaker, Thin Solid Films **411**, 1 (2002).
  - [3] P. Erhart, A. Klein, R. G. Egdell, and K. Albe, Phys. Rev. B **75**, 153205 (2007); S. Z. Karazhanov *et al.*, Phys. Rev. B **76**, 075129 (2007), and references therein.
  - [4] A. Klein, Appl. Phys. Lett. **77**, 2009 (2000).
  - [5] C. McGuinness, C. B. Stagarescu, P. J. Ryan, J. E. Downes, D. Fu, K. E. Smith, and R. G. Egdell, Phys. Rev. B **68**, 165104 (2003).
  - [6] Y. Gassenbauer, R. Schafraneck, A. Klein, S. Zafeirotas, M. Hävecker, A. Knop-Gericke, and R. Schlögl, Phys. Rev. B **73**, 245312 (2006).
  - [7] R. L. Weiher and R. P. Ley, J. Appl. Phys. **37**, 299 (1966).
  - [8] I. Hamberg, C. G. Granqvist, K. F. Berggren, B. E. Sernelius, and L. Egström, Phys. Rev. B **30**, 3240 (1984).
  - [9] H. Köstlin, R. Jost, and W. Lems, Phys. Status Solidi A **29**, 87 (1975).
  - [10] V. Christou, M. Etchells, O. Renault, P. J. Dobson, O. V. Salata, G. Beamson, and R. G. Egdell, J. Appl. Phys. **88**, 5180 (2000).
  - [11] Y. Dou, R. G. Egdell, D. S. L. Law, N. M. Harrison, and B. G. Searle, J. Phys. Condens. Matter **10**, 8447 (1998).
  - [12] M. Sachhi *et al.*, Phys. Rev. B **71**, 155117 (2005).
  - [13] J. Nordgren, G. Bray, S. Cramm, R. Nyholm, J. E. Rubensson, and N. Wassdahl, Rev. Sci. Instrum. **60**, 1690 (1989).
  - [14] J. H. Scofield, Lawrence Livermore National Laboratory Report No. UCRL-51326, 1973.
  - [15] P. A. Glans, T. Learmonth, K. E. Smith, J. Guo, A. Walsh, G. W. Watson, F. Terzi, and R. G. Egdell, Phys. Rev. B **71**, 235109 (2005).
  - [16] M. Marezio, Acta Crystallogr. **20**, 723 (1966).
  - [17] P. Hohenberg and W. Kohn, Phys. Rev. **136**, B864 (1964); W. Kohn and L. J. Sham, Phys. Rev. **140**, A1133 (1965).
  - [18] J. P. Perdew, K. Burke, and M. Ernzerhof, Phys. Rev. Lett. **77**, 3865 (1996).
  - [19] P. E. Blöchl, Phys. Rev. B **50**, 17953 (1994).
  - [20] G. Kresse and J. Furthmüller, Phys. Rev. B **54**, 11 169 (1996).
  - [21] B. Adolph, J. Furthmüller, and F. Bechstedt, Phys. Rev. B **63**, 125108 (2001).
  - [22] To compensate for the standard DFT band gap underestimation, a shift was applied to the conduction band to match the calculated optical band gap with the widely quoted 3.75 eV experimental gap.
  - [23] D. Segev and S.-H. Wei, Phys. Rev. B **71**, 125129 (2005).
  - [24] X. Nie, S.-H. Wei, and S. B. Zhang, Phys. Rev. Lett. **88**, 066405 (2002).
  - [25] J. P. Dahl and A. C. Switendick, J. Phys. Chem. Solids **27**, 931 (1966).
  - [26] D. Fröhlich, R. Kenklies, and R. Helbig, Phys. Rev. Lett. **41**, 1750 (1978).
  - [27] M. Stapelbroek and B. D. Evans, Solid State Commun. **25**, 959 (1978).
  - [28] K. R. Reyes-Gil, E. A. Reyes-Garcia, and D. Raftery, J. Phys. Chem. C **111**, 14 579 (2007).
  - [29] X. Zhang, Q. Zhang, and F. Lu, Semicond. Sci. Technol. **22**, 900 (2007).